Quark-mass dependence of two-nucleon observables

Jiunn-Wei Chen,[1,2,*] Tze-Kei Lee,[1,†] C.-P. Liu,[3,‡] and Yu-Sheng Liu[1,§]
[1]*Department of Physics and Center for Theoretical Sciences, National Taiwan University, Taipei 10617, Taiwan*
[2]*Leung Center for Cosmology and Particle Astrophysics, National Taiwan University, Taipei 10617, Taiwan*
[3]*Department of Physics, National Dong Hwa University, Shoufeng, Hualien 97401, Taiwan*
(Received 6 October 2011; published 6 November 2012)

We study the potential implications of lattice QCD determinations of the *S*-wave nucleon-nucleon scattering lengths with unphysical light quark masses. If the light quark masses are small enough such that nuclear effective field theory (NEFT) can be used to perform quark-mass extrapolations, then the leading quark-mass dependence of not only the effective range and the two-body current, but also all the low-energy deuteron matrix elements up to next-to-leading-order in NEFT can be obtained. As a proof of principle, we compute the quark-mass dependence of the deuteron charge radius, magnetic moment, polarizability, and the deuteron photodisintegration cross section using the lattice calculation of the scattering lengths at 354 MeV pion mass by the "Nuclear Physics with Lattice QCD" (NPLQCD) collaboration and the NEFT power counting scheme of Beane, Kaplan, and Vuorinen (BKV), even though it is not yet established that the 354 MeV pion mass is within the radius of convergence of the BKV scheme. Once the lattice result with quark mass within the NEFT radius of convergence is obtained, our observation can be used to constrain the time variation of isoscalar combination of *u* and *d* quark mass m_q, to help the anthropic principle study to find the m_q range that allows the existence of life, and to provide a weak test of the multiverse conjecture.

DOI: 10.1103/PhysRevC.86.054001 PACS number(s): 21.30.Fe, 21.45.Bc, 24.85.+p

I. INTRODUCTION

A very interesting aspect of lattice QCD (LQCD) calculations is that one can study the quark-mass dependence of physical observables which are otherwise hard to measure with experiments. This information can be used to constrain the time variation [1–3] of quark masses in the evolution of the universe [4–7]. It can also shed light on how finely tuned the quark masses should be [8–12] such that light nuclei can be synthesized through the usual pathway of big bang nucleosynthesis (BBN) [13,14] and make the familiar carbon-based life forms possible.

Much has been learned from the *u* and *d* quark-mass (we will work in the isosymmetric limit $m_u = m_d = m_q$) dependence of the meson and single baryon observables [15,16] through LQCD [17], chiral perturbation theory (ChPT) [18–21], and experimental data. In principle, lattice QCD can map out all the m_q dependence for these observables. However, most of the calculations are done with m_q's larger than their physical values because it requires more computing resources to work with smaller m_q. Fortunately, ChPT, which is an effective field theory (EFT) of QCD, can be used to described the m_q dependence once the unknown parameters in the theory are fixed by either the experiments or lattice data.

In the multibaryon sector, much progress has been made in LQCD in two-nucleon [22–26], nucleon-hyperon [27], triton [28,29], and α-particle [29] systems (see Ref. [30] for a brief review). However, for two-nucleon systems, so far only the *S*-wave scattering lengths have been computed with 354 MeV or heavier pion mass m_π [23]. (Note that the physical pion mass $m_\pi^{\text{phys}} \simeq 138$ MeV, and there is a one-to-one correspondence between m_π and m_q (e.g., $m_\pi \propto m_q^{1/2}$ as $m_q \to 0$). So the m_π and m_q dependencies can be converted to each other.) While it has been demonstrated that phase shift data can be described by nuclear effective field theories (NEFTs) using different power counting schemes with nice convergence at least up to ∼350 MeV center-of-mass momentum (see the brief review in the next section), it is not yet established whether the 354 MeV pion mass is within the radius of convergence of those NEFTs or not, largely because the lack of quark-mass-dependent data as inputs for the testing. In this work, we will demonstrate that given the nucleon-nucleon *S*-wave scattering lengths result within the radius of convergence, the leading quark-mass dependence of not only the effective range and the two-body current, but also all the low-energy deuteron matrix elements up to next-to-leading-order in NEFT, can be obtained.

We will focus on processes with the typical momentum $p \ll m_\pi$, such that the pions can be taken as heavy particles and integrated out of the theory. This theory is known as pionless theory [31–34]. The information of the pion dynamics in the pionful theory is now encoded in the m_π-dependent couplings of the pionless theory. It is found that all the leading m_π dependence in deuteron matrix elements in the pionless theory can be computed using the pionful theory together with the m_π dependence of the *S*-wave scattering lengths obtained from LQCD. Thus once they are fixed at m_π^{phys} their values at other pion masses are also known.

Of course, one can still work with the pionful theory. The matching is a convenient but not necessary step to take. One advantage of working with the theory without pions is that once the m_π dependence of the couplings is worked out, one can just perform the calculation in the pionless theory instead of the more complicated pionful theory.

*jwc@phys.ntu.edu.tw
†chikei@gmail.com
‡cpliu@mail.ndhu.edu.tw
§mestelqure@gmail.com

 ©2012 American Physical Society

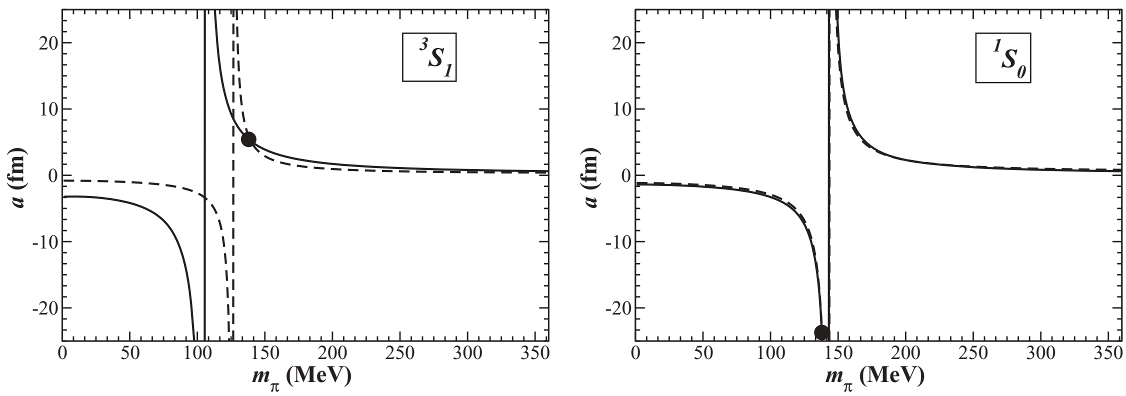

(a) (b)

FIG. 1. Scattering lengths of the (a) $^3S_1$ and (b) $^1S_0$ states versus m_π using the NLO BKV result of Eq. (8), the physical scattering length, and the scattering length computed at $m_\pi = 353$ MeV with LQCD. The dashed (solid) lines are with (without) the higher-order m_π dependence in M, f, and g_A included. The dot is the physical point.

To demonstrate this explicitly, we match the pionful theory based on Beane, Kaplan, and Vuorinen's (BKV) [35] power counting scheme to a pionless theory. This allows the matching to be done analytically. However, the method can be applied to other power schemes as well. Also, as a proof of principle, we take the 354 MeV pion mass data of Ref. [23] as inputs even though it is not clear whether this pion mass is within the radius of convergence of NEFT.

II. POWER COUNTING SCHEMES IN NUCLEAR EFFECTIVE FIELD THEORY

Currently, there are several power counting schemes for the nuclear effective theory used for multinucleon systems. Power counting means counting the power of the small expansion parameter of a Feynman diagram, such that one can organize the computation in a series expansion of this parameter. In nuclear EFT, the small expansion parameter Q is m_π/Λ and p/Λ, where Λ is the cutoff scale. Here we briefly review some popular power counting schemes.

In Weinberg's scheme [36–38] power counting is done to the potential of the Lippmann-Schwinger equation, not the diagram. The leading-order (LO) potential involves the one-pion exchange (OPE) potential and the delta function potential from contact interactions. Subtracting the infinities in the LO diagram requires higher-order operators with a high power of quark-mass insertions. Thus the result has a cutoff dependence that cannot be removed [39–41]. A similar situation happens to higher partial waves as well [41]. However, within a reasonable range of the cutoff, the scheme works well numerically with impressive fits to nucleon-nucleon (NN) scattering phase shift data at the fourth order [42–58].

The alternative scheme proposed by Kaplan, Savage, and Wise (KSW) [59,60] counts the diagrams near the nontrivial UV fixed point of the four-nucleon operators such that the cutoff dependence is removed and the diagrams of the same order are of equal size. The LO S-wave diagrams only contain nonderivative four-nucleon contact interactions, while the next-to-leading-order (NLO) contains OPE diagrams and diagrams with higher-order four-nucleon operators. However, numerically, the convergence is not good in the $^3S_1$ channel due to the singular nature of the tensor pion exchange potential at short distance $\hat{\mathbf{r}}_i\hat{\mathbf{r}}_j/r^3$, where $\mathbf{r}$ is the distance between two nucleons [61,62].

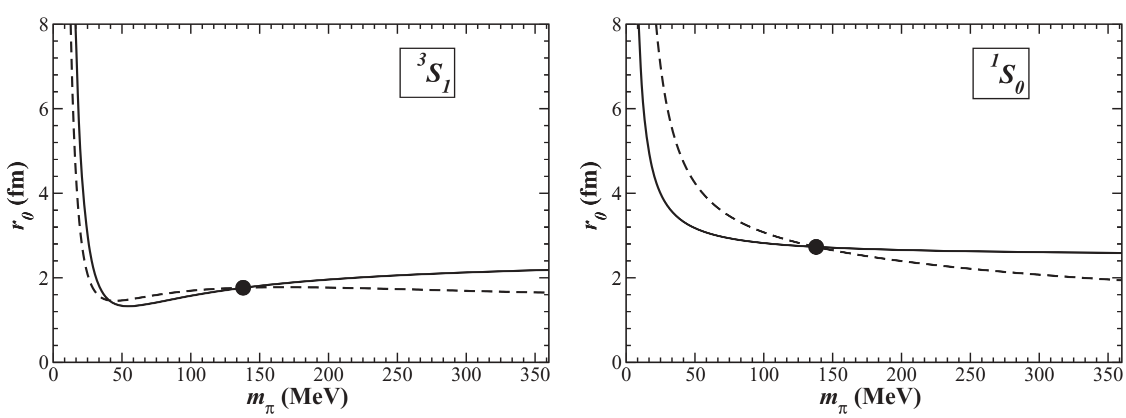

(a) (b)

FIG. 2. Effective ranges of the (a) $^3S_1$ and (b) $^1S_0$ states versus m_π using the NLO BKV result of Eq. (9). The notations are the same as in Fig. 1.

This suggests that the tensor pion exchange might not be perturbative.

In view of this problem, the tensor pion exchange is resummed at the LO in the scheme proposed by Beane, Bedaque, Savage, and van Kolck (BBSvK) [40], where the $^1S_0$ channel follows the KSW power counting while the $^3S_1$ channel follows Weinberg's power counting. It was shown that the cutoff can be removed in this scheme.

The BKV scheme [35] seeks to fix the same problem by introducing a Pauli-Villars (PV) field in the $^3S_1$ channel to remove the short distance part of the singular tensor potential. The resulting $^3S_1$ phase shift is convergent. The price to pay is that the PV mass λ is counted as the same order as m_π, but numerically it is close to the cutoff scale. However, its analytic result is very convenient to perform the matching to a pionless theory. Thus we will adopt the BKV scheme in this work.

III. QUARK MASS DEPENDENCE OF EFFECTIVE RANGE PARAMETERS

The S-wave NN scattering amplitude is

$$\mathcal{A} = \frac{4\pi}{M}\frac{1}{p\cot\delta - ip}, \tag{1}$$

where $M = 938.92$ MeV is the nucleon mass, p is the magnitude of the nucleon three-momentum in the center-of-mass (CM) frame, and δ is the S-wave phase shift. If the interaction (potential) is localized, then δ has the expansion [63,64]

$$p\cot\delta = -\frac{1}{a} + \frac{1}{2}r_0 p^2 + \cdots, \tag{2}$$

where the effective range parameters (ERPs) a and r_0 are the scattering length and the effective range, respectively. The shape parameter and higher-order terms are not shown.

In the BKV scheme, the amplitude can be expanded in powers of the small expansion parameter Q

$$\mathcal{A} = \mathcal{A}_{-1} + \mathcal{A}_0 + \mathcal{A}_1 + \cdots, \tag{3}$$

where $\mathcal{A}_n$ is of order Q^n in the expansion. Hence

$$p\cot\delta = ip + \frac{4\pi}{M\mathcal{A}_{-1}} - \frac{4\pi\mathcal{A}_0}{M\mathcal{A}_{-1}^2} + \cdots. \tag{4}$$

A. Working in the BKV scheme as an explicit example

The BKV scheme is the same as the KSW scheme in the $^1S_0$ channel, but different in the $^3S_1$ channel. The LO amplitude of channel i arises from the diagrams in Fig. 5 of Ref. [59]

$$\mathcal{A}_{-1}^{(i)} = \frac{-C_0^{(i)}}{\left[1 + \frac{C_0^{(i)}M}{4\pi}(\mu + ip)\right]}, \tag{5}$$

where C_0 is the LO four-nucleon nonderivative coupling which is independent of m_q. The NLO amplitude arises from the diagrams in Fig. 6 of Ref. [59] plus the associated diagrams with the PV fields

$$\begin{aligned} \mathcal{A}_0^{(^1S_0)} &= \mathcal{A}_{0,a}^{(^1S_0)} + \mathcal{A}_{0,b}^{(^1S_0)}(m_\pi), \\ \mathcal{A}_0^{(^3S_1)} &= \mathcal{A}_{0,a}^{(^3S_1)} + \mathcal{A}_{0,b}^{(^3S_1)}(m_\pi) - \epsilon\mathcal{A}_{0,b}^{(^3S_1)}(\lambda), \end{aligned} \tag{6}$$

where ϵ is introduced to keep track of the difference between the BKV and the KSW power counting. $\epsilon = 1$ gives the BKV result while $\epsilon = 0$ gives the KSW result

$$\begin{aligned} \mathcal{A}_{0,a}^{(i)} &= \frac{-\left(C_2^{(i)}p^2 + C_{0,0}^{(i)}\right)}{\left[1 + \frac{C_0^{(i)}M}{4\pi}(\mu + ip)\right]^2}, \\ \mathcal{A}_{0,b}^{(i)}(m_\pi) &= \frac{-D_2^{(i)}m_\pi^2}{\left[1 + \frac{C_0^{(i)}M}{4\pi}(\mu + ip)\right]^2} + \left(\frac{g_A^2}{2f^2}\right)\left[-1 + \frac{m_\pi^2}{4p^2}\ln\left(1 + \frac{4p^2}{m_\pi^2}\right)\right] \\ &\quad + \frac{g_A^2}{f^2}\left(\frac{m_\pi M\mathcal{A}_{-1}}{4\pi}\right)\left\{-\frac{(\mu + ip)}{m_\pi} + \frac{m_\pi}{2p}\left[\tan^{-1}\left(\frac{2p}{m_\pi}\right) + \frac{i}{2}\ln\left(1 + \frac{4p^2}{m_\pi^2}\right)\right]\right\} \\ &\quad + \frac{g_A^2}{2f^2}\left(\frac{m_\pi M\mathcal{A}_{-1}}{4\pi}\right)^2\left\{1 - \left(\frac{\mu + ip}{m_\pi}\right)^2 + i\tan^{-1}\left(\frac{2p}{m_\pi}\right) - \frac{1}{2}\ln\left(\frac{m_\pi^2 + 4p^2}{\mu^2}\right)\right\}. \end{aligned} \tag{7}$$

where g_A is the pion nucleon coupling constant, f is the pion decay constant, and we have imposed isospin symmetry by setting $m_u = m_d$ and neglecting the electromagnetic interaction. $C_{0,0}$ is an NLO operator with the same structure as C_0. D_2 is a nonderivative four-nucleon coupling with one insertion of m_q (or m_π^2), and C_2 is a two-derivative four-nucleon operator that is independent of m_q. μ is the renormalization scale, and we used dimensional regularization and the power-divergence subtraction procedure (PDS) [59] to renormalize the theory. These amplitudes are manifestly renormalization-scale independent order-by-order in the EFT expansion.

Expanding the right-hand side of Eq. (4) in powers of p, we have the matching for the spin singlet and triplet scattering lengths

$$\begin{aligned} \frac{1}{a^{(^1S_0)}} &= \gamma^{(^1S_0)} - \frac{M}{4\pi}\left(\gamma^{(^1S_0)} - \mu\right)^2\left(D_2^{(^1S_0)}m_\pi^2 + C_{0,0}^{(^1S_0)}\right) \\ &\quad + \frac{g_A^2 M}{8\pi f^2}\left[m_\pi^2\log\left(\frac{\mu}{m_\pi}\right) + \left(\gamma^{(^1S_0)} - m_\pi\right)^2 - \left(\gamma^{(^1S_0)} - \mu\right)^2\right], \end{aligned}$$

$$\frac{1}{a^{(^3S_1)}} = \gamma^{(^3S_1)} - \frac{M}{4\pi}\left(\gamma^{(^3S_1)} - \mu\right)^2 \left[D_2^{(^3S_1)}\left(m_\pi^2 - \epsilon\lambda^2\right) + C_{0,0}^{(^3S_1)}\right] + \frac{g_A^2 M}{8\pi f^2}\left[m_\pi^2 \log\left(\frac{\mu}{m_\pi}\right) + \left(\gamma^{(^3S_1)} - m_\pi\right)^2 - \left(\gamma^{(^3S_1)} - \mu\right)^2\right] - \epsilon\frac{g_A^2 M}{8\pi f^2}\left[\lambda^2 \log\left(\frac{\mu}{\lambda}\right) + \left(\gamma^{(^3S_1)} - \lambda\right)^2 - \left(\gamma^{(^3S_1)} - \mu\right)^2\right], \tag{8}$$

where $\gamma^{(i)} = \mu + 4\pi/MC_0^{(i)}$ is the LO inverse scattering length. We perform the expansion around the physical pion mass $m_\pi^{\text{phys}} \simeq 138$ MeV, so $\gamma^{(i)}$ takes the physical value $1/a_{\text{phys}}^{(i)}$. To fix $D_2^{(i)}$ and $C_{0,0}^{(i)}$ we just need $1/a^{(i)}$ computed at another m_π other than m_π^{phys}.

The matching for effective ranges gives

$$r_0^{(^1S_0)} = \frac{MC_2^{(^1S_0)}\left(\mu - \gamma^{(^1S_0)}\right)^2}{2\pi} + \frac{g_A^2 M}{12\pi f^2}\left[6\left(\frac{\gamma^{(^1S_0)}}{m_\pi}\right)^2 - 8\frac{\gamma^{(^1S_0)}}{m_\pi} + 3\right]$$

$$r_0^{(^3S_1)} = \frac{MC_2^{(^3S_1)}\left(\mu - \gamma^{(^3S_1)}\right)^2}{2\pi} + \frac{g_A^2 M}{12\pi f^2}\left\{6\left(\frac{\gamma^{(^3S_1)}}{m_\pi}\right)^2 - 8\frac{\gamma^{(^3S_1)}}{m_\pi} + 3 - \epsilon\left[6\left(\frac{\gamma^{(^3S_1)}}{\lambda}\right)^2 - 8\frac{\gamma^{(^3S_1)}}{\lambda} + 3\right]\right\}. \tag{9}$$

Unlike the scattering lengths, no lattice data are needed to study the quark-mass dependence of the effective ranges since $C_2^{(i)}$ can be fixed by $r_0^{(i)}$ at m_π^{phys}.

Note that the ϵ terms in $1/a^{(^3S_1)}$ and $r_0^{(^3S_1)}$ are m_π independent, so they can be absorbed into counterterms $C_{0,0}^{(^3S_1)}$ and $C_2^{(^3S_1)}$. Therefore, the KSW and BKV schemes give the same m_π dependence to ERP's at NLO.

In summary, Eqs. (8) and (9) can be parametrized as

$$\frac{1}{a^{(i)}} = \overline{\gamma}^{(i)} - d_2^{(i)} m_\pi^2 + \frac{g_A^2 M}{8\pi f^2}\left[m_\pi^2 \log\left(\frac{\mu}{m_\pi}\right) + (\gamma^{(i)} - m_\pi)^2\right],$$

$$r_0^{(i)} = c_2^{(i)} + \frac{g_A^2 M}{12\pi f^2}\left[6\left(\frac{\gamma^{(i)}}{m_\pi}\right)^2 - 8\frac{\gamma^{(i)}}{m_\pi}\right]. \tag{10}$$

The physical $a^{(i)}$ and $r_0^{(i)}$ ($a_{\text{phys}}^{(^3S_1)} = 5.423 \pm 0.005$ fm, $r_{0,\text{phys}}^{(^3S_1)} = 1.764 \pm 0.002$ fm, $a_{\text{phys}}^{(^1S_0)} = -23.714 \pm 0.003$ fm, $r_{0,\text{phys}}^{(^1S_0)} = 2.73 \pm 0.03$ fm) fix $c_2^{(i)}$, and a combination of $\overline{\gamma}^{(i)}$ and $d_2^{(i)}$. We only need an LQCD calculation of $a^{(i)}$ at different m_π to get the leading m_π dependence for $a^{(i)}$ and $r_0^{(i)}$.

Currently, the smallest m_π that $a^{(i)}$ is computed on the lattice is 353.7 ± 2.1 MeV [23]. The calculation yields $a^{(^3S_1)} = 0.63 \pm 0.74$ fm, $a^{(^1S_0)} = 0.63 \pm 0.50$ fm. As mentioned above, though it is not clear whether this pion mass is within the radius of convergence of any NEFT. We choose to work with these data as a proof of principle. The central values yield the solid curves in Figs. 1 and 2.

Since BKV did not publish their next-to-next-to-leading-order (NNLO) result, we only explore the size of NNLO corrections by including the m_π dependence of M, f, and g_A,, which is extracted from the lattice data [65,66] to Eqs. (8) and (9). This yields the dashed curves in Figs. 1 and 2. The $a^{(^3S_1)} \to \infty$ position can shift by $\sim 20\%$ in m_π due to higher-order corrections, while the corrections to $a^{(^1S_0)}$ are much smaller. When $m_\pi \gtrsim 100$ MeV, $r_0^{(i)} \simeq 2$ fm and is insensitive to m_π. Again, we warn the readers that our error analysis is far from complete and the analysis here should be viewed as a proof of principle.

The analytic structure of the scattering amplitude, Eq. (1), is that there are two cuts from $p = im_\pi/2$ to $i\infty$ and from $p = -im_\pi/2$ to $-i\infty$. There is a $^3S_1$ bound state for $m_\pi = 106$ to 142 MeV (with $\lambda = 750$ MeV, but the range remains the same for $\lambda = 500$ to 1000 MeV) and a $^1S_0$ bound state for $m_\pi = 144$ to 165 MeV. The corresponding binding energies are shown in Fig. 3. This result can be understood by examining the scattering amplitude in the effective range expansion. By keeping only the scattering length and effective range in Eq. (2), the amplitude of Eq. (1) has two poles

$$p = \frac{i}{r_0}\left(1 \pm \sqrt{1 - \frac{2r_0}{a}}\right). \tag{11}$$

If $a > 0$, the solution with smaller $|p|$ is $p = \frac{i}{r_0}(1 - \sqrt{1 - \frac{2r_0}{a}})$. The bound state exists when $0 < \frac{2r_0}{a} < 1$.

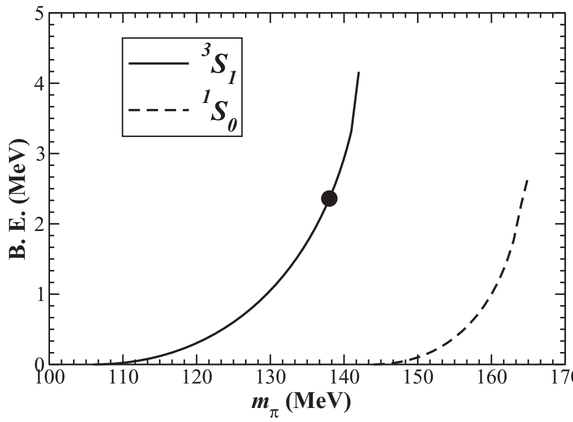

FIG. 3. Bound state (whenever it exists) binding energy (B.E.) versus m_π for $^3S_1$ (solid line) and $^1S_0$ (dashed line). The notations are the same as in Fig. 1.

However, if $a < 0$, the solution with smaller $|p|$ is $p = \frac{i}{r_0}(1 - \sqrt{1 - \frac{2r_0}{a}})$. Since $\frac{2r_0}{a} < 0$, the pole does not correspond to a bound state. The other pole $p = \frac{i}{r_0}(1 + \sqrt{1 - \frac{2r_0}{a}})$ (for both positive and negative a) is of the order of the ultraviolet cutoff scale $1/r_0$, which is usually hidden in the cut starting at $p = im_\pi/2$. Thus the bound-state range is $0 < 2r_0 < a$, which is close to the ranges seen in Fig. 3. Furthermore, the maximum binding momentum is i/r_0, or the maximum binding energy is $1/(Mr_0^2)\sim 6$ MeV for $r_0 \sim 2.5$ fm.

With the current lattice input, this theory does not have a two-nucleon bound state in the chiral ($m_q \to 0$, or equivalently $m_\pi \to 0$) limit. However, different power countings can lead to different conclusions [23]. This might indicate that $m_\pi = 354$ MeV is not within the radius of convergence of the m_π expansion for these theories. It is important to have both higher-order EFT calculations and lattice results at lower quark masses to decide this radius of convergence in m_π before a firm conclusion about the deuteron binding energy in the chiral limit can be drawn.

B. A support for multiverse?

It is curious that in our result m_π^{phys} is so close to the upper bound of m_π where the deuteron is bounded. If this result still holds in more reliable determinations with lattice inputs of smaller quark masses, then if m_π^{phys} were 5% bigger, then there would not have been a deuteron at all. This makes it much harder for primordial nuclear synthesis to form light nuclei through the usual pathways and might eventually make life impossible. This interesting fine-tuning implies that our universe sits near the edge of the parameter space where life can exist. In Ref. [67], it was argued that this was not a fine-tuning, but a natural case if the multiverse exists: In a multiverse, which is an ensemble of many universes including ours, the majority of the universes do not allow life to exist since it requires lots of conditions to be satisfied. Thus the peak of the m_q distribution in this multiverse will be more likely to sit outside the parameter space where life is possible. In that case, the tail of the distribution goes across this parameter space and then one finds that most of the universes that permit life are near the edge of the parameter space. Thus if the multiverse exists, without fine-tuning, our universe should live near the edge of the parameter space where life is possible (called the catastrophic boundary by the authors of Ref. [67]). It is interesting to note that our case of the deuteron bound state is consistent with this pattern, similar to the example of the cosmological constant whose value is close to the allowed range obtained by Weinberg through the anthropic principle [68,69] and several examples worked out by the authors of Ref. [67]. Although we do not consider this as a sharp test of the multiverse conjecture because the conjecture cannot be falsified even if the physical m_q is far away from the edge of the allowed parameter space, it is still interesting to see whether there are cases consistent with this conjecture.

IV. MATCHING BETWEEN THE THEORY WITH AND WITHOUT PIONS

We are interested in using the theory without pions to describe low-energy processes (where $p < m_\pi$ so pions can be integrated out) at nonphysical m_π. The matching between the pionful and pionless EFT's at those m_π gives the m_π dependence of the couplings in the pionless theory. Those couplings are the ERP's of NN scattering mentioned above and current operators when coupled to external currents.

We can classify the nonderivative single-nucleon (one-body) current operators by how they transform in the spin-isospin space: the scalar-scalar operator ($N^\dagger N$), scalar-vector operator ($N^\dagger \tau_i N$), vector-scalar operator ($N^\dagger \sigma_i N$), and vector-vector operator ($N^\dagger \sigma_i \tau_j N$), where $\sigma_i(\tau_i)$ acts on the spin(isospin) space and the spacial indexes $i, j = 1, 2, 3$. The nonderivative scalar-scalar and scalar-vector operators originate from matrix elements of the quark level operators $\overline{q}\gamma_0 q$ and $\overline{q}\gamma_0\tau_i q$. They do not have two-body currents due to vector current conservation. For vector-scalar currents, they can originate from matrix elements of the isoscalar quark axial operator $\overline{q}\gamma_i\gamma_5 q$ or the magnetic part of the vector current $\overline{q}\gamma_i q$, so the corresponding two body-currents exist. For vector-vector currents, the corresponding quark level operator is $\overline{q}\gamma_i\gamma_5\tau_j q$ and the two-body currents (called Gamow-Teller operators) also exist.

From matching the isoscalar magnetic current between the theory with and without pions, we conclude that the vector-scalar two-body currents do not depend on pion mass at the leading order [70]. The matching of the two-body Gamow-Teller operator [71,72] yields

$$\begin{aligned} L_{\text{GT}} = l_{\text{GT}} &- \frac{\kappa_1 g_A^2 m_\pi^2}{2\gamma^2 f^2} \log\left(\frac{m_\pi}{m_\pi + 2\gamma}\right) \\ &- \frac{\kappa_1 g_A^2}{6\gamma f^2 m_\pi^2 (m_\pi + 2\gamma)}\left[6m_\pi^4 + m_\pi^2\left(9m_\pi - \frac{4}{a^{(^1S_0)}}\right)\gamma \right. \\ &- 2m_\pi\gamma^2\left(m_\pi - \frac{5}{a^{(^1S_0)}}\right) \\ &\left. -2\gamma^3\left(5m_\pi + \frac{6}{a^{(^1S_0)}}\right) + 12\gamma^4\right], \end{aligned} \tag{12}$$

where l_{GT} is m_π independent, $\gamma = (1 - \sqrt{1 - 2r_0^{(^3S_1)}/a^{(^3S_1)}})/r_0^{(^3S_1)}$ is the deuteron binding momentum, and κ_1 is the single nucleon coupling (for the isovector magnetic current, κ_1 is the isovector nucleon magnetic moment; for weak coupling, κ_1 is proportional to g_A). There is no unknown parameter in the m_π-dependent term.

V. MORE QUARK-MASS DEPENDENCE OF TWO-NUCLEON OBSERVABLES

In this section we apply the m_π-dependent couplings in the pionless EFT, which was worked out in the previous sections, to compute several physical observables involving deuterons.

A. Deuteron properties

The deuteron charge radius has the expression [33]

$$\langle r_d^2 \rangle = \langle r_{N,0}^2 \rangle + \frac{1}{8\gamma^2 (1-\gamma\rho_d)}, \tag{13}$$

where the isoscalar charge radius of the nucleon $\sqrt{\langle r_{N,0}^2 \rangle} = 0.79 \pm 0.01$ fm and $\rho_d = r_0^{(^3S_1)}$. As expected, the deuteron charge radius $\sqrt{\langle r_d^2 \rangle}$ is set by the inverse binding momentum $1/\gamma$ when the nucleon charge radius is negligible. The m_π dependence for $m_\pi = 125$–141 MeV (where the deuteron is bounded) is shown in Fig. 4.

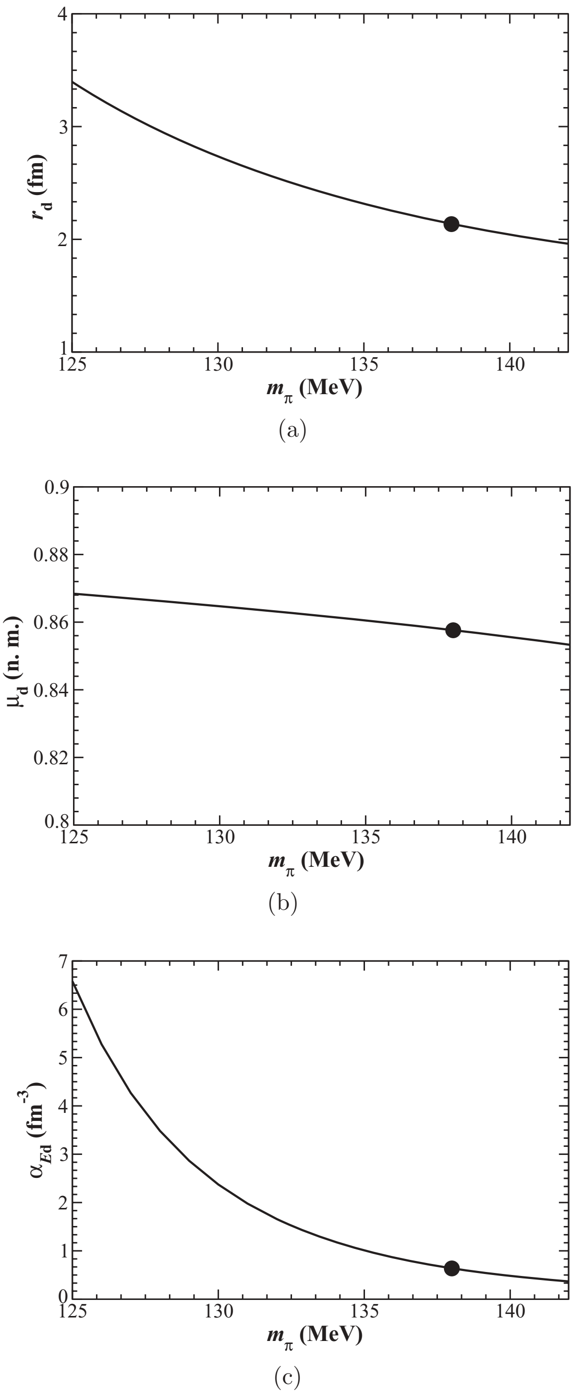

FIG. 4. (a) Deuteron charge radius r_d, (b) magnetic moment μ_d, and (c) electric polarizability α_{Ed}, versus m_π. The dots are the physical points.

The deuteron magnetic moment is [33]

$$\mu_M = \frac{e}{2M}(2\kappa_0 + \gamma L_{V-S}), \tag{14}$$

where $\kappa_0 = 0.44$ is the nucleon isoscalar magnetic moment in units of nuclear magneton (N.M.) and the vector-scalar two-body current L_{V-S} is m_π independent. Neither the one-nucleon nor the two-nucleon contribution is sensitive to m_π. The sum is also shown in Fig. 4.

The deuteron polarizability is computed as [33]

$$\alpha_{E,0} = \frac{\alpha M}{32\gamma^4(1-\gamma\rho_d)}, \tag{15}$$

$\alpha = 1/137$ is the fine-structure constant. It has a strong m_π dependence as is shown in Fig. 4.

B. Reaction: $np \leftrightarrow d\gamma$

The process $np \leftrightarrow d\gamma$ is relevant for BBN. Its cross section is proportional to the wave-function overlap between the initial and final states. Since the deuteron size $1/\gamma$ is very sensitive to m_π near $m_\pi^{\rm phys}$, the cross section also changes dramatically in this region.

The total cross section for $np \to d\gamma$ is [73,74]

$$\sigma(np \to d\gamma) = \frac{4\pi\alpha(\gamma^2+p^2)^3}{\gamma^3 M^4 p}\left[|\tilde{X}_{M1}|^2 + |\tilde{X}_{E1}|^2\right], \tag{16}$$

where p is the magnitude of the momentum of each nucleon in the CM frame. The electric dipole ($E1$) transition yields

$$|\tilde{X}_{E1}|^2 = \frac{p^2 M^2 \gamma^4}{(\gamma^2+p^2)^4}[1 + \gamma\rho_d + (\gamma\rho_d)^2 + \cdots]. \tag{17}$$

The magnetic dipole ($M1$) transition yields

$$|\tilde{X}_{M1}|^2 = \frac{\kappa_1^2\gamma^4\left(\frac{1}{a^{(^1S_0)}} - \gamma\right)^2}{\left(\frac{1}{a^{(^1S_0)2}} + p^2\right)(\gamma^2+p^2)^2} \times \left[1 + \gamma\rho_d - r_0^{(^1S_0)} \frac{\left(\frac{\gamma}{a^{(^1S_0)}} + p^2\right)p^2}{\left(\frac{1}{a^{(^1S_0)2}} + p^2\right)\left(\frac{1}{a^{(^1S_0)}} - \gamma\right)} - \frac{L_{\rm GT}}{\kappa_1}\frac{M}{2\pi}\frac{\gamma^2+p^2}{\frac{1}{a^{(^1S_0)}} - \gamma}\right]. \tag{18}$$

The Gamow-Teller two-body current $L_{\rm GT} = -4.513\,{\rm fm}^2$ at $m_\pi = m_\pi^{\rm phys}$ is fitted from the measured cross section $\sigma^{\rm expt} = 334.2 \pm 0.5$ mb [73] using incident neutrons of speed $|v| = 2200$ m/s. The m_π dependence of $L_{\rm GT}$ is shown in Eq. (2). The isovector nucleon magnetic moment $\kappa_1 = 2.35 - g_A^2 M(m_\pi - m_\pi^{\rm phys})/(2\pi f^2)$, where we applied the m_π dependence calculated from ChPT [21]. The cross section of the reverse process

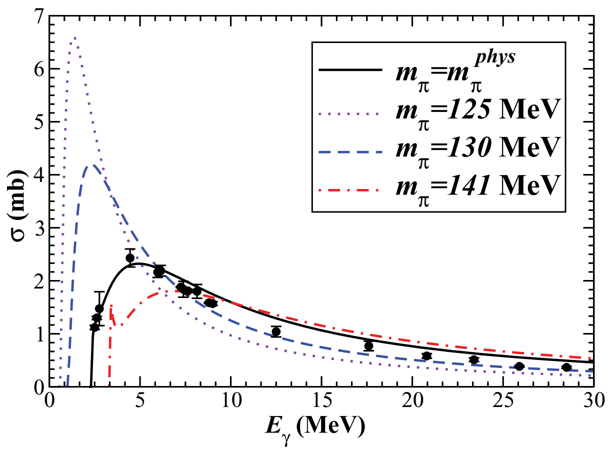

FIG. 5. (Color online) The cross section for $\gamma d \to np$ as a function of the incident photon energy in megaelecton volts. The solid curve is for the physical m_π, while the dotted, dot-dashed, and dashed curves are for $m_\pi = 125$, 130, and 141 MeV, respectively.

with deuteron being at rest is

$$\sigma(\gamma d \to np) = \frac{2M(E_\gamma - B)}{3E_\gamma^2}\sigma(np \to d\gamma), \tag{19}$$

where E_γ is the incident photon energy. This deuteron photodisintegration cross section for $m_\pi = 125$–141 MeV is shown in Fig. 5.

VI. CONCLUSION

We studied the potential implications of LQCD determinations of the S-wave nucleon-nucleon scattering lengths with unphysical light quark masses. If the light quark masses are small enough such that NEFT can be used to perform quark-mass extrapolations, then the leading quark-mass dependence of not only the effective range and the two-body current, but also all the low-energy deuteron matrix elements up to next-to-leading-order in NEFT, can be obtained.

As a proof of principle, we computed the quark-mass dependence of the deuteron charge radius, magnetic moment, polarizability, and the deuteron photodisintegration cross section using the the lattice calculation of the scattering lengths at 354 MeV pion mass by the "Nuclear Physics with Lattice QCD" (NPLQCD) collaboration and the NEFT power counting scheme of Beane, Kaplan, and Vuorinen, even though it is not yet established that the 354 MeV pion mass is within the radius of convergence of the BKV scheme. Once the lattice result with quark mass within the NEFT radius of convergence is obtained, our observation can be used to constrain the time variation of the isoscalar combination of u and d quark mass m_q to help the anthropic principle study to find the m_q range that allows the existence of life, and to provide a weak test of the multiverse conjecture.

Previously, BBN was used to constrain the time variation of the isoscalar light quark mass [75,76]. In Ref. [75], the quark-mass dependence on S-wave nucleon-nucleon scattering lengths was extracted from the same lattice data [23] as we did but with a different NEFT. The quark-mass dependence of other observables such as the binding energy of ^{3}He, ^{3}H, and ^{4}He was assumed to come solely from the nucleon-nucleon scattering lengths. In Ref. [76], the quark-mass dependence of light nuclei binding energies was derived from a potential model. Both Refs. [75,76] can benefit from our observation that the leading quark-mass dependence of the effective ranges and the two-body currents can be obtained with no extra input.

ACKNOWLEDGMENTS

We thank Martin Savage for providing us the formulas describing the LQCD m_π dependence of M, f, and g_A. This work is supported by the NSC under Grant Nos. NSC99-2112-M-002-010-MY3 (JWC, TKL, and YSL) and NSC98-2112-M-259-004-MY3 (CPL), the NCTS, and the NTU-CASTS of ROC.

[1] P. A. M. Dirac, Nature (London) **139**, 323 (1937).
[2] J. K. Webb, V. V. Flambaum, C. W. Churchill, M. J. Drinkwater, and J. D. Barrow, Phys. Rev. Lett. **82**, 884 (1999).
[3] J. K. Webb *et al.*, Phys. Rev. Lett. **87**, 091301 (2001).
[4] V. V. Flambaum and R. B. Wiringa, Phys. Rev. C **76**, 054002 (2007).
[5] S. R. Beane and M. J. Savage, Nucl. Phys. A **713**, 148 (2003).
[6] S. R. Beane and M. J. Savage, Nucl. Phys. A **717**, 91 (2003).
[7] E. Epelbaum, U. G. Meissner, and W. Gloeckle, Nucl. Phys. A **714**, 535 (2003).
[8] V. V. Flambaum and E. V. Shuryak, Phys. Rev. D **65**, 103503 (2002).
[9] J. P. Kneller and G. C. McLaughlin, Phys. Rev. D **68**, 103508 (2003).
[10] J. P. Kneller and G. C. McLaughlin, Phys. Rev. D **70**, 043512 (2004).
[11] S. J. Landau, M. E. Mosquera, and H. Vucetich, Astrophys. J. **637**, 38 (2006).
[12] T. Dent, S. Stern, and C. Wetterich, Phys. Rev. D **76**, 063513 (2007).
[13] R. A. Alpher, H. Bethe, and G. Gamow, Phys. Rev. **73**, 803 (1948).
[14] S. Burles, K. M. Nollett, and M. S. Turner, Astrophys. J. **552**, L1 (2001).
[15] E. E. Scholz, PoS (LAT2009) 005.
[16] C. Alexandrou, PoS (LAT2010) 001.
[17] K. G. Wilson, Phys. Rev. D **10**, 2445 (1974).
[18] J. Gasser and H. Leutwyler, Ann. Phys. (NY) **158**, 142 (1984).
[19] J. Gasser and H. Leutwyler, Nucl. Phys. B **250**, 465 (1985).
[20] E. E. Jenkins and A. V. Manohar, Phys. Lett. B **255**, 558 (1991).
[21] V. Bernard, N. Kaiser, and U. G. Meissner, Int. J. Mod. Phys. E **4**, 193 (1995).
[22] M. Fukugita, Y. Kuramashi, M. Okawa, H. Mino, and A. Ukawa, Phys. Rev. D **52**, 3003 (1995).
[23] S. R. Beane, P. F. Bedaque, K. Orginos, and M. J. Savage, Phys. Rev. Lett. **97**, 012001 (2006).
[24] N. Ishii, S. Aoki, and T. Hatsuda, Phys. Rev. Lett. **99**, 022001 (2007).
[25] S. Aoki, T. Hatsuda, and N. Ishii, Comput. Sci. Dis. **1**, 015009 (2008).

[26] S. R. Beane *et al.* (NPLQCD Collaboration), Phys. Rev. D **81**, 054505 (2010).
[27] S. R. Beane, P. F. Bedaque, T. C. Luu, K. Orginos, E. Pallante, A. Parreno, and M. J. Savage (NPLQCD Collaboration), Nucl. Phys. A **794**, 62 (2007).
[28] S. R. Beane *et al.*, Phys. Rev. D **80**, 074501 (2009).
[29] T. Yamazaki, Y. Kuramashi, and A. Ukawa (f. C. Collaboration), Phys. Rev. D **81**, 111504 (2010).
[30] M. J. Savage, arXiv:1010.2282.
[31] D. B. Kaplan, Nucl. Phys. B **494**, 471 (1997).
[32] P. F. Bedaque and U. van Kolck, Phys. Lett. B **428**, 221 (1998).
[33] J. W. Chen, G. Rupak, and M. J. Savage, Nucl. Phys. A **653**, 386 (1999).
[34] S. R. Beane and M. J. Savage, Nucl. Phys. A **694**, 511 (2001).
[35] S. R. Beane, D. B. Kaplan, and A. Vuorinen, Phys. Rev. C **80**, 011001 (2009).
[36] S. Weinberg, Phys. Lett. B **251**, 288 (1990).
[37] S. Weinberg, Nucl. Phys. B **363**, 3 (1991).
[38] S. Weinberg, Phys. Lett. B **295**, 114 (1992).
[39] D. B. Kaplan, M. J. Savage, and M. B. Wise, Nucl. Phys. B **478**, 629 (1996).
[40] S. R. Beane, P. F. Bedaque, M. J. Savage, and U. van Kolck, Nucl. Phys. A **700**, 377 (2002).
[41] A. Nogga, R. G. E. Timmermans, and U. van Kolck, Phys. Rev. C **72**, 054006 (2005).
[42] C. Ordonez and U. van Kolck, Phys. Lett. B **291**, 459 (1992).
[43] C. Ordonez, L. Ray, and U. van Kolck, Phys. Rev. Lett. **72**, 1982 (1994).
[44] U. van Kolck, Phys. Rev. C **49**, 2932 (1994).
[45] C. Ordonez, L. Ray, and U. van Kolck, Phys. Rev. C **53**, 2086 (1996).
[46] J. L. Friar, D. Huber, and U. van Kolck, Phys. Rev. C **59**, 53 (1999).
[47] M. C. M. Rentmeester, R. G. E. Timmermans, J. L. Friar, and J. J. de Swart, Phys. Rev. Lett. **82**, 4992 (1999).
[48] V. Bernard, N. Kaiser, and U. G. Meissner, Nucl. Phys. A **615**, 483 (1997).
[49] E. Epelbaum, W. Gloeckle, and U. G. Meissner, Nucl. Phys. A **671**, 295 (2000).
[50] E. Epelbaum, H. Kamada, A. Nogga, H. Witala, W. Gloeckle, and Ulf-G. Meissner, Phys. Rev. Lett. **86**, 4787 (2001).
[51] E. Epelbaum, A. Nogga, W. Gloeckle, H. Kamada, U. G. Meissner, and H. Witala, Eur. Phys. J. A **15**, 543 (2002).
[52] E. Epelbaum, W. Gloeckle, and U. G. Meissner, Eur. Phys. J. A **19**, 401 (2004).
[53] E. Epelbaum, W. Glockle, and U. G. Meissner, Nucl. Phys. A **747**, 362 (2005).
[54] D. R. Entem and R. Machleidt, Phys. Lett. B **524**, 93 (2002).
[55] D. R. Entem and R. Machleidt, Phys. Rev. C **66**, 014002 (2002).
[56] D. R. Entem and R. Machleidt, Phys. Rev. C **68**, 041001 (2003).
[57] M. Pavon Valderrama and E. Ruiz Arriola, Phys. Rev. C **74**, 054001 (2006).
[58] M. Pavon Valderrama and E. Ruiz Arriola, Phys. Rev. C **74**, 064004 (2006); **75**, 059905(E) (2007).
[59] D. B. Kaplan, M. J. Savage, and M. B. Wise, Nucl. Phys. B **534**, 329 (1998).
[60] D. B. Kaplan, M. J. Savage, and M. B. Wise, Phys. Lett. B **424**, 390 (1998).
[61] S. Fleming, T. Mehen, and I. W. Stewart, Phys. Rev. C **61**, 044005 (2000).
[62] S. Fleming, T. Mehen, and I. W. Stewart, Nucl. Phys. A **677**, 313 (2000).
[63] H. A. Bethe, Phys. Rev. **76**, 38 (1949).
[64] H. A. Bethe and C. Longmire, Phys. Rev. **77**, 647 (1950).
[65] R. G. Edwards *et al.* (LHPC Collaboration), Phys. Rev. Lett. **96**, 052001 (2006).
[66] S. R. Beane, P. R. Bedaque, K. Orginos, and M. J. Savage (NPLQCD Collaboration), Phys. Rev. D **73**, 054503 (2006).
[67] R. Bousso, L. J. Hall, and Y. Nomura, Phys. Rev. D **80**, 063510 (2009).
[68] S. Weinberg, Phys. Rev. Lett. **59**, 2607 (1987).
[69] H. Martel, P. R. Shapiro, and S. Weinberg, Astrophys. J. **492**, 29 (1998).
[70] D. B. Kaplan, M. J. Savage, and M. B. Wise, Phys. Rev. C **59**, 617 (1999).
[71] M. Butler and J. W. Chen, Nucl. Phys. A **675**, 575 (2000).
[72] M. Butler, J. W. Chen, and X. Kong, Phys. Rev. C **63**, 035501 (2001).
[73] J. W. Chen and M. J. Savage, Phys. Rev. C **60**, 065205 (1999).
[74] G. Rupak, Nucl. Phys. A **678**, 405 (2000).
[75] P. F. Bedaque, T. Luu, and L. Platter, Phys. Rev. C **83**, 045803 (2011).
[76] M.-K. Cheoun, T. Kajino, M. Kusakabe, and G. J. Mathews, Phys. Rev. D **84**, 043001 (2011).